

# Kinetic Assessment of Manganese Using Magnetic Resonance Imaging in the Dually Perfused Human Placenta *In Vitro*

by Richard K. Miller,\* Donald R. Mattison,<sup>†</sup> Maurice Panigel,<sup>‡</sup> Toni Ceckler,\* Robert Bryant,\* and Peter Thomford<sup>†</sup>

The transfer and distribution of paramagnetic manganese was investigated in the dually perfused human placenta *in vitro* (using 10, 20, 100  $\mu$ M Mn with and without  $^{54}\text{Mn}$ ) using magnetic resonance imaging (MRI) and conventional radiochemical techniques. The human placenta concentrated  $^{54}\text{Mn}$  rapidly during the first 15 min of perfusion and by 4 hr was four times greater than the concentrations of Mn in the maternal perfusate, while the concentration of Mn in the fetal perfusate was 25% of the maternal perfusate levels. Within placenta, 45% of the  $^{54}\text{Mn}$  was free in the 100,000g supernatant, with 45% in the 1,000g pellet. The magnetic field dependence of proton nuclear spin-lattice relaxation time ( $T_1$ ) in placental tissue supports this Mn binding. Mn primarily affected the MRI partial saturation rather than spin-echo images of the human placenta, which provided for the separation of perfusate contributions from those produced by Mn. The washout of the Mn from the placenta was slow compared with its uptake, as determined by MRI. Thus, Mn was concentrated by the human placenta, but transfer of Mn across the placenta was limited in either direction. These studies also illustrate the opportunity for studies of human placental function using magnetic resonance imaging as a noninvasive biomarker.

## Introduction

The movement of xenobiotic agents across the placenta from mother to conceptus has been difficult to assess in the human because of inaccessibility. Such toxicokinetic assessments are essential for understanding the effects of agents on the developing organism as well as the pregnant woman. Biomarkers of effect have been the classical means for establishing damage to the conceptus. It is hoped, however, that biomarkers of exposure may be just as important if not more important to establishing populations that may or may not be at risk for having abnormal pregnancies. Unfortunately, to date, the assessment of maternal blood and urine have been the primary fluids analyzed. More recently amniotic fluid has also been screened. Yet, the kinetics of practically all compounds is limited by the snapshot

assessment for kinetic analysis at or about the time of delivery, when samples of cord blood, placenta, amniotic fluid, and fetal hair are easily obtained. Advances in two different arenas have provided the opportunity to evaluate the characteristics of human placental transfer for different agents using a dually perfused human placental preparation *in vitro* and also using the noninvasive technique of magnetic resonance imaging (MRI). These techniques have been combined to determine the pharmacokinetics and patterns of distribution within the human placenta for the paramagnetic ion manganese.

Manganese can be neurotoxic in chronically exposed miners (1-4). These men were affected by severe disorders of speech, posture, and gait, as well as sexual impotence. Mn is normally found in plasma from pregnant and nonpregnant women at levels of 1.5 to 2.0 ng/mL (5). There are no reports concerning human exposures to excess levels of Mn during pregnancy. A number of animal teratology studies using Mn during organogenesis have not shown malformations (two rat studies, two hamster studies, one mouse study, and one rabbit study) (4,6,7). In another earlier study by Ferm (8), where the maternal lethal dose was 35 mg/kg, IV  $\text{MnCl}_2$  produced a dose-related increase in resorptions, but no malformations were reported. Behavioral studies in progeny exposed *in utero* have not been reported.

\*Departments of Obstetrics/Gynecology, Pharmacology and Biophysics, Environmental Health Sciences Center, University of Rochester, School of Medicine and Dentistry, 601 Elmwood Avenue, Rochester, NY 14642.

<sup>†</sup>Department of Obstetrics/Gynecology, Division of Reproductive Toxicology, University of Arkansas for Medical Sciences, 4301 West Markham, Little Rock, AR 77205 and the National Center for Toxicological Research, Jefferson, AR 72079.

<sup>‡</sup>Department of Reproductive Biology, University of Paris VI, Paris, France 75005.



A

FIGURE 1. Visualization of Mn in the pregnant cynomolgus monkey. (A) Pregnant primate before injection of Mn. The image is a spin-echo ( $T_R = 600$  msec;  $T_E = 40$  msec). Note that the anterior and posterior lobes of the placenta are poorly distinguished from the uterus. The maternal kidney is observable. *Continued on next page.*



B

FIGURE 1. *Continued.* (B) Pregnant primate from Fig. 1A, but 17 min after injection of Mn. Note the enhanced image of the placenta, which is now separated from the uterine tissue and the fetus. The maternal kidney image is also enhanced. From Thomford et al. (23).

Certainly, Mn has the potential to be toxic to the developing CNS if sufficient Mn does reach the fetus.

The human investigations reported here are based upon previous studies by Kay and Mattison (9) using MRI *in utero*, where Mn was selectively concentrated

in the placenta of the rhesus monkey (Figs. 1A,B); increases in Mn were not noted in the uterus or in the fetus itself. Such selectivity in placental accumulation with a minimal passage to the conceptus was proposed as a possible tool for visualizing the placenta selectively

using noninvasive techniques. It is hoped that by combining MRI with *in vitro* human placental perfusion studies, one may determine directly the kinetics and possible toxicity of Mn by using sensitive methods for analysis, e.g., radiochemical detection, and comparing these data with the evaluation of manganese distribution via MR analysis.

## Methods

### *In Vitro* Human Placental Perfusion

An extended dual recirculating human placental preparation was used in this study. The isolated human lobular perfusion is based upon the original description by Schneider, Panigel, and Dancis (10) as modified and adapted for extended perfusion by Miller et al. (11). The same physiological, morphological, and biochemical criteria were used in these Mn studies as were previously described (11). Major modifications of the perfusion chamber and system were necessary to conform to the dimensions of the magnetic resonance imaging equipment as noted in Figures 2 and 3. Of special note is approximately 12 feet of tubing required to connect the chamber with the fetal and maternal pumps. In addition, there are heating tubes in the perfusion chamber to maintain the tissue at temperatures of  $36^{\circ}\text{C} \pm 1$ . The internal diameter of the perfusion chamber was maintained; however, the height was reduced by 35%. French 5 umbilical catheters were used in both the fetal and maternal circulations. Flow rates were 15 mL/min on the maternal side and 3 mL/min on the fetal side. The fetal pressure was  $34 \pm 4$  mm Hg.

The fetal perfusates were composed of tissue culture medium M199 (Difco, Detroit, MI) with heparin (25 IU/mL, A. H. Robbins), glucose (2.0 g/L), dextran 40 (fetal:

30 g/L, maternal: 7.5 g/L, Sigma), and gentamicin (50 mg/L, A. H. Robbins). The fetal perfusate was gassed with 95%  $\text{N}_2$ /5%  $\text{CO}_2$  and recirculated following the collections of the first 40 mL of perfusate. The maternal perfusate was gassed with 95%  $\text{O}_2$ /5%  $\text{CO}_2$  and also was recirculated following the collection of the first 60 mL of perfusate. The recirculating volumes in the maternal and fetal circuits were 190 and 65 mL, respectively. During the first 2 hr (the control period), two perfusate samples were collected from the fetal reservoir and from the maternal arterial port every half hour for analysis of  $\text{P}_{\text{O}_2}$ ,  $\text{P}_{\text{CO}_2}$ , pH, glucose, and lactate. At 2 hr, and every 4 hr thereafter, perfusates in both circuits were exchanged for fresh perfusates. Sodium bicarbonate was added to the perfusates when the pH was less than 7.32.

Fetal capillary integrity was monitored by measuring the volume in the fetal reservoir during the perfusion. The sensitivity of this method is  $\pm 2$  mL, which reflects a measure of 2 mL/hr as the limit of detection for leak in these studies. Volume loss greater than 10 mL/hr from the fetal circulation has been associated with an inability of the capillaries to retain inulin and indicates damage (12). Fetal arterial pressure was measured using a Graeco standard aneroid sphygmomanometer.

Blood gases and pH were measured using an Instrumentation Laboratories Model 1302 pH/blood gas analyzer. Maternal  $\text{O}_2$  delivery, tissue  $\text{O}_2$  consumption, and net  $\text{O}_2$  transfer to the fetal circulation were calculated according to the methods of Wier and Miller (13).

### Manganese Assessments

In the first series of experiments,  $^{54}\text{Mn}$  plus  $\text{MnCl}_2$  (10, 20, or 100  $\mu\text{M}$ ) was added together to either the fetal or maternal reservoirs after a 2-hr control perfu-

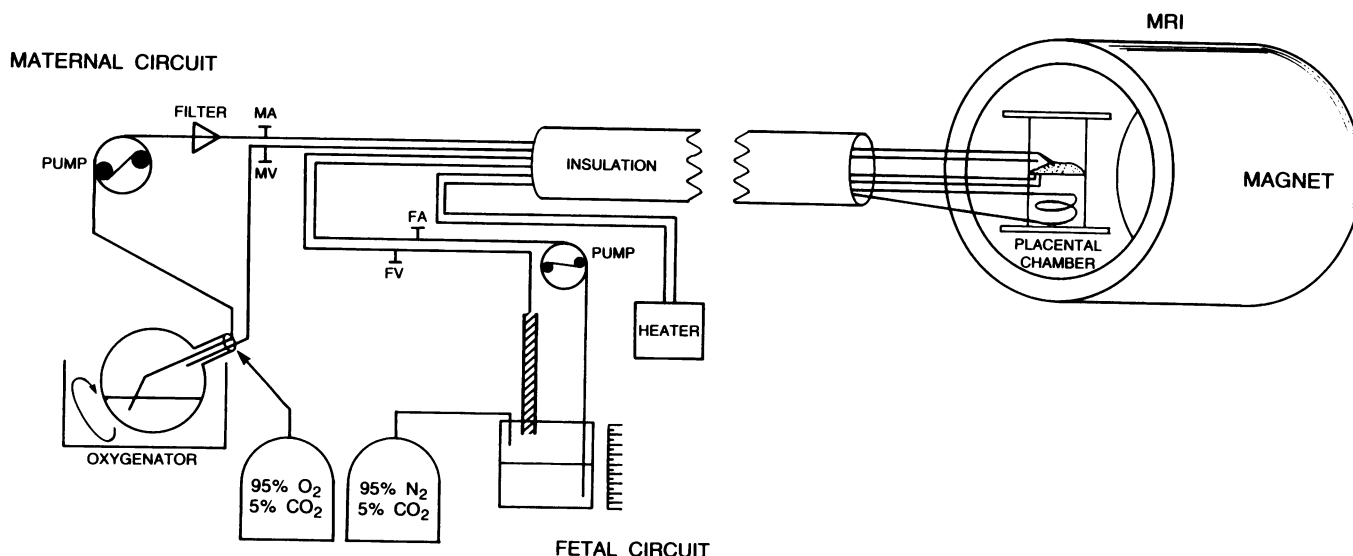
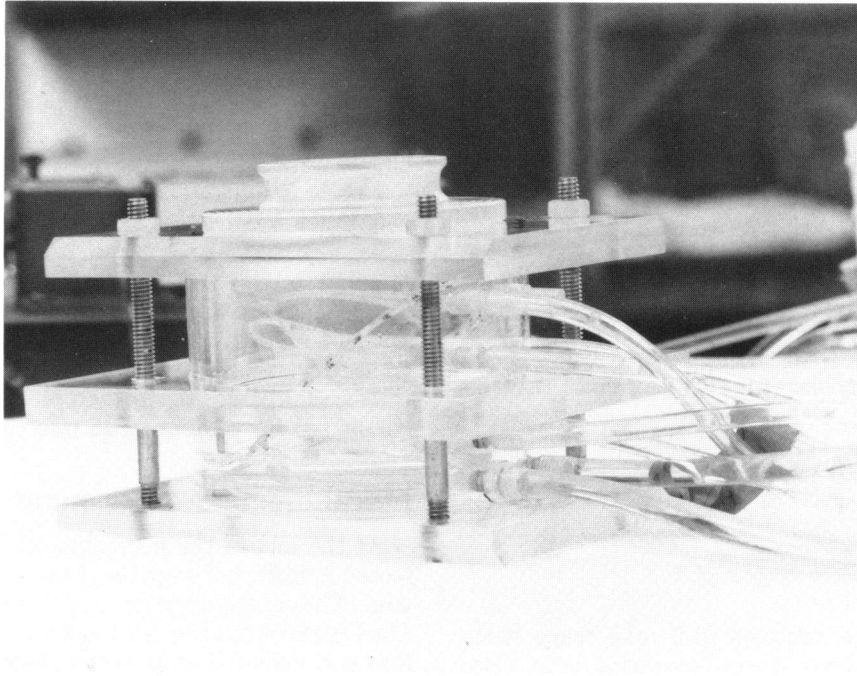
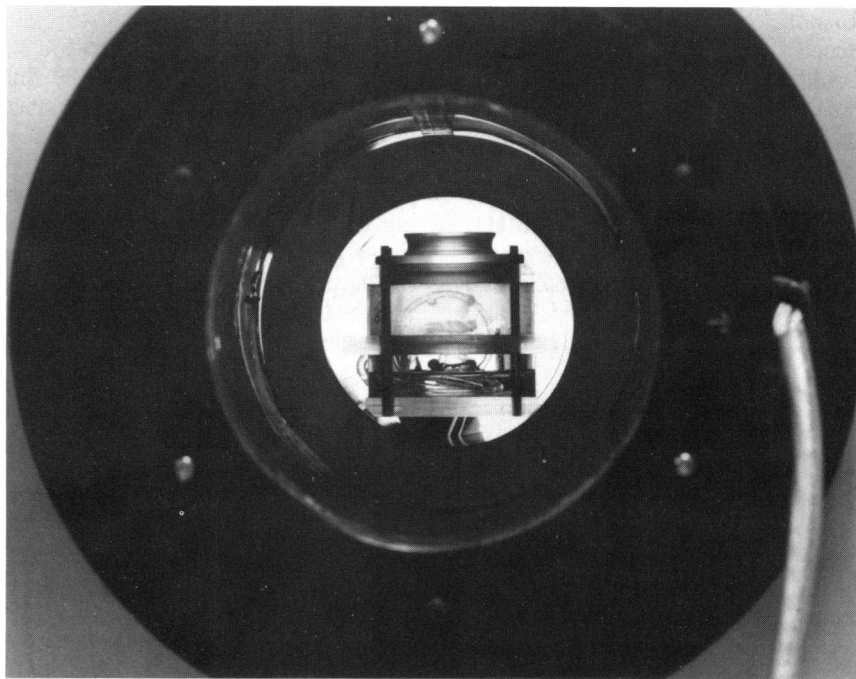


FIGURE 2. Schematic diagram of the perfusion apparatus at the MRI unit. MA = maternal artery; MV = maternal vein; FA = fetal artery; FV = fetal vein.



A



B

FIGURE 3. Perfusion chamber modified for MRI use. (A) Perfusion chamber attached to "umbilical cord," which contains two maternal tubes, two fetal tubes, and two heating tubes. Insulation material surrounds the three inflow tubes spanning the 12 feet from the pumps to the MRI magnet (shown in 3B). All materials are constructed of nonmagnetic materials, e.g., aluminum, teflon, plastic. Note heating coils in bottom of chamber. (B) Perfusion chamber within the core of the 2.0 tesla General Electric MRI magnet at the University of Rochester's Magnetic Resonance Imaging Facility.



Table 1. Placental perfusate ratios for Mn.

Time, hr	Perfusate, $\mu\text{mole/mL}$	Tissue perfusate ratio, $\mu\text{mole/g}/\mu\text{mole/mL}$
Maternal administration		
0.25	21.1	1.18
2.00	14.4	$4.6 \pm 0.05$
4.00	8.5	$3.9 \pm 0.3$
Fetal administration		
2.00	9.4	$4.2 \pm 0.4$

Table 2. Distribution of Mn within placental and fluid compartments following *in vitro* perfusion.<sup>a</sup>

Administration route	Time, hr	% Mn in compartment		
		Maternal	Placental	Fetal
Maternal	2	35.0	56.0	8.5
Fetal	2	6.5	47.0	46.0

<sup>a</sup> Average of three placental perfusions.

sion period. Perfusate samples (0.2 mL) were withdrawn from the maternal artery, maternal vein, fetal artery, and fetal vein simultaneously at 1 min intervals for the first 20 min, then at 5 min intervals until 60 min. After 60 min following the addition of the Mn, samples were collected every 15 min.

Mn was measured directly during the experiment via an in-line MR probe (Praxis II Pulsed Nuclear Magnetic Resonance Analyzer, San Antonio, TX) in the maternal artery for maternal additions of Mn or in the fetal vein for fetal additions of Mn. The Praxis II is a 0.25 tesla permanent magnet with the sample coil and a radio frequency (RF) pulse generator operating at 10.7 MHz. After the experiment, the other collections were measured in the Praxis. For  $^{54}\text{Mn}$ , samples were collected from all four ports and analyzed via a Nuclear Chicago gamma counter with a 48% efficiency for  $^{54}\text{Mn}$ .

## Magnetic Resonance Imaging of the Mn in the Human Placenta

A mobile human placental perfusion unit was developed for use in the Magnetic Resonance Imaging Facility at the University of Rochester. A General Electric 2.0 tesla MRI unit was used with conventional spin-echo spin warp imaging sequences to acquire the images. For tissue imaging with Mn, the optimized relaxation time ( $T_R$ ) was 500 msec, and the excitation time ( $T_E$ ) was 25 msec. Studies maximizing for tissue imaging without Mn had a  $T_R$  of 900 msec and a  $T_E$  of 75 msec. Images were usually constructed from four repetitions. Only imaging was performed on this unit. Studies were conducted for periods of 15 min to 10 hr.

## Morphological Assessment

At the end of the perfusion, chorionic villi were collected in different regions of the perfused placental lobule. These specimens were immediately fixed in MacDowell's fixative and refrigerated until impregnation and embedding in epoxy resin. Ultra thin sections were examined with a Phillips electron microscope.

## Results

The transfer and distribution of paramagnetic manganese was investigated in 20 dually perfused human placentae *in vitro* using magnetic resonance and conventional radiochemical techniques. Following the bolus injection of Mn into the maternal reservoir, the human placental perfused lobule concentrated Mn rapidly during the first 15 min of perfusion and by 4 hr was four times greater than the concentrations of Mn in the maternal perfusate (Table 1). Similar concentrations of Mn within the placenta were possible if Mn was presented from the fetal circulation (Table 1).

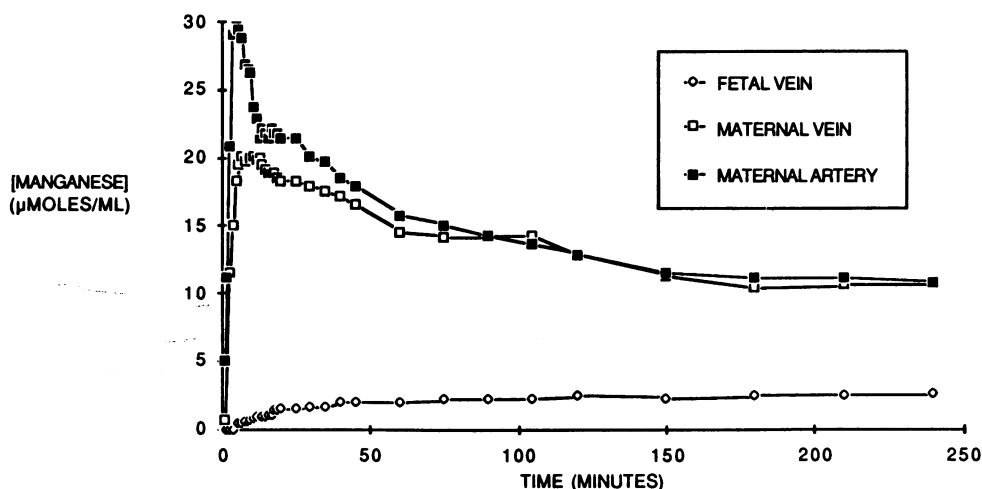


FIGURE 4. Placental perfusion of Mn as measured by  $^{54}\text{Mn}$  when added to the maternal circuit. The total length of this experiment was 6 hr, where the first 2 hr were the control periods. The Mn was added following transfusion at 2 hr, and collections of fluids followed for an additional 4 hr. Maternal arterial concentrations of Mn appeared at 9 min, while no peak was noted in the fetal vein for Mn.

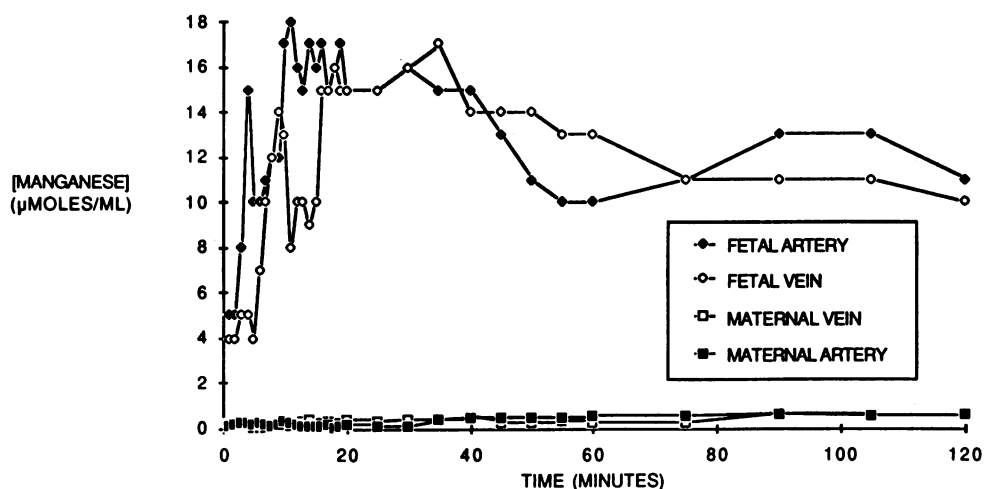


FIGURE 5. Placental perfusion of Mn as measured by  $^{54}\text{Mn}$  when added to the fetal circuit. The total length of this experiment was 4 hr, where the first 2 hr were control. The Mn was added following transfusion at 2 hr, and collections of fluids followed for an additional 2 hr. Peak concentrations in the fetal artery for Mn occurred approximately 17 min after the addition of the Mn to the fetal circuit. During the 2 hr of perfusion, 7.4% of the total Mn transited to the maternal circulation; however, at 2 hr the concentration of Mn in the maternal circuit was less than 10% of the fetal [Mn].

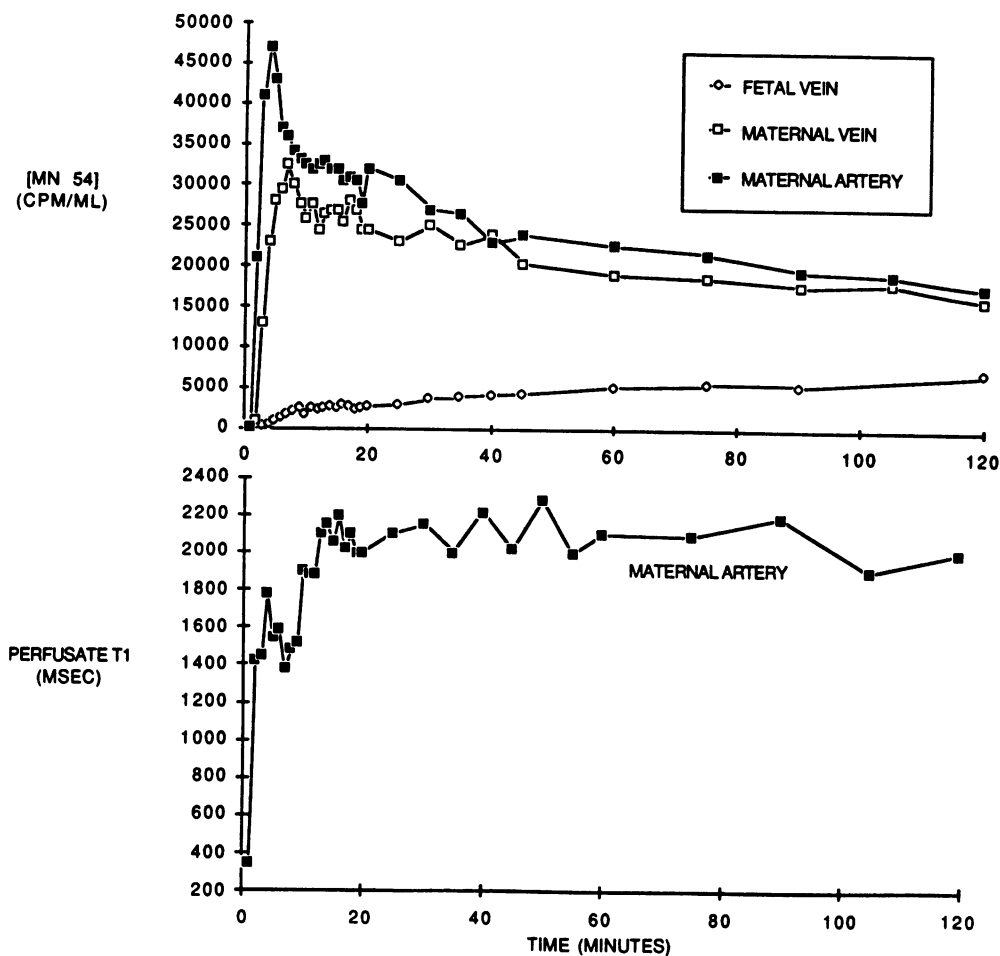


FIGURE 6. Comparison of radiochemical and MR spectrometric analyses of Mn under perfusion conditions in the human placental lobule. In the upper graph, the radioactivity measurements were determined after the experiment was completed; in the lower graph, a Praxis MR unit with a modified flow cell directly measured the [Mn] in the maternal artery during the course of the experiment. The relaxation time ( $T_1$ ) is known to be inversely related to the concentration of Mn as is apparent in this figure.

Less than 10% of the total Mn is transferred in either direction to the fetal or maternal compartments during the first 2 hr of Mn exposure (Table 2). After 4 hr of perfusion following addition of Mn to the maternal reservoir, the concentration of Mn in the fetal perfusate was 25% of the maternal perfusate levels as measured via  $^{54}\text{Mn}$  (Fig. 4). Equilibration between the maternal and fetal circuits did not occur following addition of Mn to the fetal reservoir, even though the placenta did concentrate the Mn (Fig. 5). Addition of 100  $\mu\text{mole/mL}$  of Mn to the maternal circuit did not saturate the amount contained within the placenta or its percentage of total Mn added to the maternal perfusate. Interestingly, there was a smaller percentage of the Mn transferred to the fetal compartment than noted for 10 or 20  $\mu\text{mole/mL}$ .

Within placentae, 45% of the  $^{54}\text{Mn}$  was free in the cytosol, with the remainder being predominantly in the 1000g pellet (43%) (Table 3). The MRI magnetic field dependence of water proton relaxation time ( $T_1$ ) is dominated by the nonmanganese contributions at the concentrations used in these studies; however, a rise in rate in the 20 MHz region supports the concept that a significant fraction of Mn (II) ion is rotationally immobilized or samples a local environment of high viscosity.

The radiochemical and magnetic relaxation rates were directly compared to determine the sensitivity of analysis (Fig. 6). The relaxation rates in the maternal arterial perfusates were proportional to the amount of Mn as determined by  $^{54}\text{Mn}$  measurements in the same experiment.

Mn primarily affected the MRI partial saturation rather than spin-echo images of the human placenta. The Mn enhanced the image intensity of the perfused lobule, which is centrally located as expected for a manganese-induced reduction of  $T_1$  for this region (Fig. 7). Note the peripheral tissues are low intensity, are not perfused, and thus must be low in Mn concentration. In the upper portion of Figure 7, which is an inverted image of Figure 3B, the low intensity circles represent fluid flowing through the heating tubes. Similar low intensity areas are noted for the fetal vasculature, since fluids flowing through vessels appear dark upon MR imaging. During washout of the Mn, the high intensity of the placental lobule persisted for at least 4 hr, even after the maternal and fetal perfusates contained nearly undetectable amounts of Mn. Thus, the Mn is not completely cleared from the placenta for extended periods,

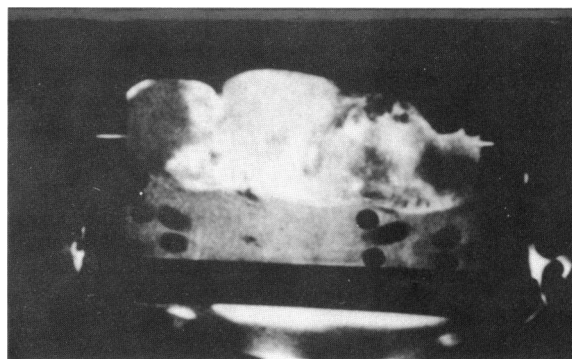


FIGURE 7. Cross-sectional view of a dually perfused human placental lobule. The central, high intensity region is enhanced by the presence of Mn in the maternal perfusate. The Mn is also concentrated in the placental tissue itself. Note the darker lateral tissue which is not being perfused with the Mn. This image represents an inverted cross-section of Fig. 3B, when a placenta would be present in the chamber. The black circles in the top of the image represent the heating coils in the amniotic fluid chamber equivalent. This image was obtained via a General Electric 2.0 tesla MRI unit with a spin-echo spin warp sequence. The repetition rate was 500 msec and the echo delay was set for 25 msec. Data acquisition used 256 phase encode steps, 1K data points using quadrature detection per step. The image data were processed to a  $512 \times 512$  matrix. The final pixel resolution was 120 mm/512.

which provides for an opportunity to perform repeated scans of the tissue without having to add additional Mn. In the  $T_2$  weighted images, only the effect of perfusion with a perfusate containing minimal red blood cells demonstrated any change in tissue image. Both sets of image acquisition parameters permitted visualization of vasculature; however, contrast between tissue and vessels was better for the  $T_1$ -weighted images ( $T_R/T_E$ , 500/25 msec) with Mn present.

Ultrastructural screening of the trophoblast and fetal endothelium of chorionic villi sampled at the end of the 4 and 2 hr of dual perfusion demonstrated the integrity of the constituents of the placental zone of maternal/fetal exchange (Fig. 8A,C) as previously established for human placental perfusions (14). In most areas of the tissue examined, the trophoblast ultrastructure maintains a normal appearance of the cellular organelles and membranes (Fig. 8A). The fetal capillaries also keep their normal ultrastructural aspect. Some of these capillaries show red blood cells remaining in the perfusate. The endothelial ultrastructure, as well as the neighboring villus stromal constituents and trophoblastic basement membrane, appear normal (Fig. 8C). In the trophoblast covering of a few placental villi, however, some changes in the microvilli, the endoplasmic reticulum cisternae, and the mitochondria have been observed (Fig. 8B). There were no alterations in glucose utilization, lactate production, oxygen consumption, or transfer or fetal volume loss during the course of these kinetic studies. It is not yet possible to state without further investigation if these ultrastructural changes are due to the morphological heterogeneity of the troph-

Table 3. Cellular distribution of Mn in the human placenta following maternal administration.

Cell fraction*	% of total $^{54}\text{Mn}$
Nuclear	42.6 $\pm$ 3.5
Mitochondria	5.3 $\pm$ 1.1
Microsomes	2.4 $\pm$ 0.2
Supernatant	45.4 $\pm$ 4.2
Recovery	95.7

\* Nuclear fraction represents the 1000g pellet; mitochondria fraction represents the 10,000g pellet; microsome fraction represents the 100,000g pellet; supernatant represents the 100,000g supernatant.



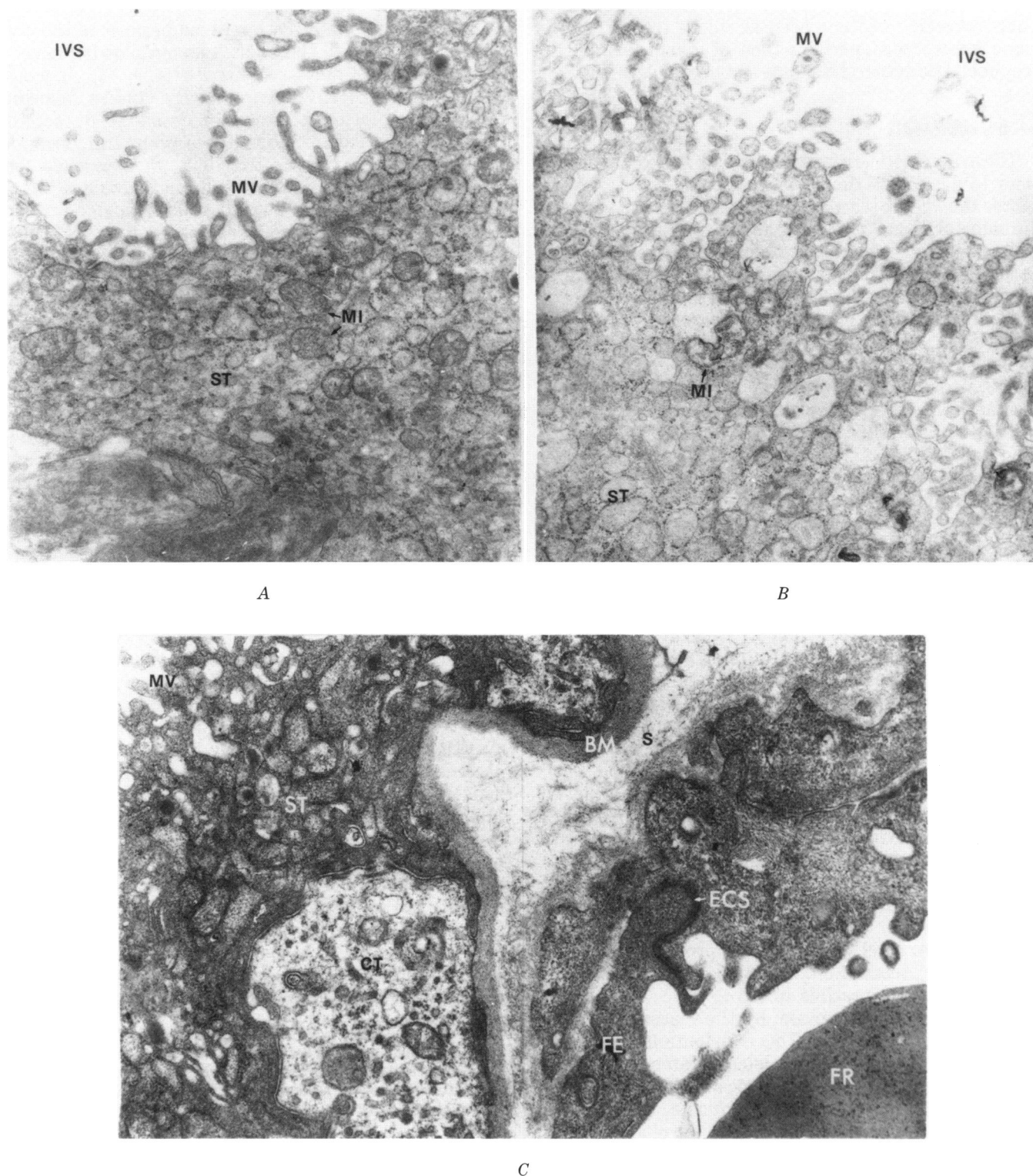


FIGURE 8. Electron micrographs of perfused human placenta. (A) Syncytiotrophoblast covering of a placental villus after 4 hr of Mn (20  $\mu$ mole/mL), total perfusion, 6 hr. (B) Syncytiotrophoblast from the same placental lobule as in Fig. 7A, but from a different region. Note invaginations of the crypts and the less distinct limits of the mitochondria. (C) The constituents of the placenta maternal/fetal exchange region after 2 hr of perfusion with manganese chloride (20  $\mu$ mole/mL), total perfusion, 4 hr. BM = basement membrane; CL = capillary lumen; CR = microcrypt; CT = cytotrophoblast; ECJ = endothelial cell junction; FE = fetal endothelium; FR = fetal red blood cell; IVS = maternal intervillous space; MI = mitochondria; MV = microvilli; S = stroma; ST = syncytiotrophoblast.

oblast covering of the placental villous tree or due, in some areas, to a specific action of manganese on the trophoblastic cytoarchitecture and organelles (Fig. 8C).

## Discussion

These studies were undertaken for two primary reasons: to determine the kinetics of Mn transfer into and across the human placenta and to establish the potential for using MRI and paramagnetic ions for enhancing the visualization of the human placenta. A few reports have used MRI for examining pregnant women (15–21); however, these studies have primarily evaluated pregnancies with suspected birth defects or other serious compromises. Functional studies have not been undertaken in the human at this time *in utero*. There have been other *in vitro* human tissue fragment studies with both myometrium and trophoblast (22,23) as well as both *in vitro* and *in vivo* subhuman primate studies (9,23) using MRI and Mn.

*In utero*, both for the human and the subhuman primate, it has been difficult to separate the adjacent tissue (placenta and myometrium) because the MR relaxation times ( $T_1$ , spin-lattice and  $T_2$ , spin-spin) are quite similar. Thus, it becomes difficult to separate maternal and fetal tissue at this interface—the implantation site (9,23). Previous *in vitro* studies have also demonstrated that human placental fragments do concentrate Mn. The Mn in the tissue shortens the proton spin relaxation times and enhances the contrast of the image. Relative Mn uptake can be followed by observing changes in MRI contrast as more of the paramagnetic ion accumulates in the tissue, as noted in Figures 6 and 7. Thus, dynamic noninvasive measures of function (e.g., blood flow, transport, and tissue concentration) can be achieved with sequential analysis. Mn enhances proton relaxation in the perfused tissue making it possible to delineate the perfused region. This enhancement of the trophoblast has been especially useful in visualizing the fetal circulation, as moving ions in fluids appear low intensity upon MRI. Thus, the tissue is high intensity and the vessels are low intensity (studies in progress). Imaging may allow for determining patterns of fetal circulation *in utero* as is now possible *in vitro*.

The kinetics of Mn uptake by the placenta is quite rapid, as noted in Table 2. This distribution among maternal and fetal circulations demonstrates that Mn is not rapidly transferred to the opposite circuit, whether added to the maternal or fetal perfusate. It should be noted that Mn is primarily localized in the placenta itself (Table 3). Such concentration of Mn in the placenta is certainly consistent with all previous investigations *in vitro* with human tissue and with the monkey studies *in utero*. These current human studies also are in agreement with the monkey studies, demonstrating the limited transfer of Mn to the fetal circulation. These studies with Mn are in contrast to gadolinium DPTA (Gd-DPTA), which rapidly appears in the fetal circulation and in the fetal bladder of the monkey (24).

Gd-DPTA is currently approved as a contrast agent

for MRI, while Mn is not approved because of the neurotoxicity of Mn in the adult human following chronic exposure and in neonatal animal studies (4). It would be important to have neurotoxicity studies following prenatal exposure to Mn in animals to determine whether Mn in sufficient quantities enters the conceptus and produces damage to the CNS. It is possible that only at maternal toxic doses will Mn be toxic to the *in utero* developing CNS. Future studies should evaluate the kinetics of Mn bound to chelators, e.g., DPTA, to determine the tissue enhancement characteristics as well as toxicity phenomenon.

When Mn is compared to inulin, vitamin  $B_{12}$ , and cadmium under similar conditions, there is comparability among the transfer of these compounds, which is quite slow compared with antipyrine, amino acids, oxygen, tritiated water, phenytoin or zinc (12,13,25–27). With the exception of inulin, Mn, vitamin  $B_{12}$ , and cadmium are bound to placental proteins, and such binding appears to retard the movement across the placenta into the opposite circuit. Also, as noted for phenytoin and tritiated water (26), manganese can be seen to move from the perfused lobule radially or along septae into nonperfused lobules. With time, nonperfused tissue does accumulate these compounds depending upon channeling and relative affinity of the tissue for the compound.

Thus, Mn is concentrated in the human placenta under *in vitro* human placental perfusion conditions, whether presented from the maternal or fetal circuit. In addition, less than 10% of the total amount of Mn added appears in the opposite circuit. Such uptake of Mn by the human placenta can be used selectively by MRI since Mn is a paramagnetic ion. The placenta can be selectively imaged due to the concentration of Mn in the trophoblast. For these acute studies no clearly identifiable signs of toxic response have been determined. Perhaps longer periods of exposure may be necessary to assess the toxicity of Mn in the human placenta. Such studies demonstrate the potential for MRI as a noninvasive technique for studying functional and structural changes during pregnancy, as has been previously demonstrated only at delivery (27) where tissue levels of metals, as well as structural evaluations, have been performed.

The authors acknowledge Jeanette Dabinett-Zavislan and Diane Rohack for their technical assistance in conducting the perfusion experiments. The electron microscopic evaluations performed by Jeanette Panigel are also acknowledged. This research team is appreciative of the assistance provided by the Labor/Delivery Staff at Strong Memorial Hospital at the University of Rochester, especially the dedication of Barbara Massaro. These studies were supported in part by NIH grants ES02774, ES01247, and CA40699.

## REFERENCES

1. Penalver, R. Manganese poisoning. *Ind. Med. Surg.* 24: 1–7 (1955).
2. Schuler, P., Oyanguen, H., Maturana, V., Valenzuela, A., Cruz, E., Plaza, V., Schmidt, E., and Haddad, R. Manganese poisoning. *Ind. Med. Surg.* 26: 167 (1957).
3. Mena, I., Marin, O., Fuenzalida, S., and Cotzias, G. C. Chronic manganese poisoning. *Neurology* 17: 128–136 (1967).

4. Barlow, S. M., and Sullivan, F. M. Reproductive Hazards of Industrial Chemicals. Academic Press, New York, 1982.
5. Hambridge, K., and Droegemueller, W. Changes in plasma and hair concentrations of zinc, copper, chromium, and manganese during pregnancy. *Obstet. Gynecol.* 44: 666-672 (1974).
6. Kimmel, C. A., Butcher, R. E., Vorhees, C. V., and Schumacher, H. J. Metal-salt potentiation of salicylate-induced teratogenesis and behavioral changes in rats. *Teratology* 10: 293-300 (1974).
7. Hanlon, D., Gale, T., and Ferm, V. Permeability of the Syrian hamster placenta to manganous ions during early embryogenesis. *J. Reprod. Fertil.* 44: 109-112 (1975).
8. Ferm, V. The teratogenic effects of metals on mammalian embryos. *Adv. Teratol.* 5: 51-75 (1972).
9. Kay, H. H., and Mattison, D. R. Magnetic resonance imaging in nonhuman primates. In: *Animal Models in Fetal Medicine* (P. W. Nathanielsz, Ed.), Perinatology Press, Ithaca, 1986, pp. 269-323.
10. Schneider, H., Panigel, M., and Dancis, J. Transfer across the perfused human placenta of antipyrine, sodium and leucine. *Am. J. Obstet. Gynecol.* 114: 822-828 (1972).
11. Miller, R. K., Wier, P. J., Maulik, D., and di Sant'Agnese, P. A. Human placenta in vitro: Characterization during 12 hours of dual perfusion. *Contrib. Gynecol. Obstet.* 13: 77-84 (1985).
12. Wier, P. J., Miller, R. K., Maulik, D., and di Sant'Agnese, P. A. Bidirectional transfer of alpha-aminoisobutyric acid by the perfused human placental lobule. *Trophoblast Res.* 1: 37-54 (1984).
13. Wier, P. J., and Miller, R. K. Oxygen transfer as an indicator of perfusion variability in the isolated human placental lobule. *Contrib. Gynecol. Obstet.* 13: 127-131 (1985).
14. di Sant'Agnese, P. A., Demesy-Jensen, K., Miller, R. K., Wier, P. J., and Maulik, D. Long term human placental lobule perfusion—an ultrastructural study. *Trophoblast Res.* 2: 549-560 (1987).
15. Cohen, J. M., Weinreb, J. C., Lowe, T. W., and Brown, C. MR imaging of a viable full-term abdominal pregnancy. *Am. J. Roentgenol. Radium Ther. Nucl. Med.* 145: 407-408 (1985).
16. Johnson, I. R., Symonds, E. M., Kean, D. M., Worthington, B. S., Pipkin, F. B., Hawkes, R. C., and Gynegell, M. Imaging the pregnant human uterus with nuclear magnetic resonance. *Am. J. Obstet. Gynecol.* 148: 1136-1139 (1984).
17. Lowe, T. W., Weinreb, J., Santos-Ramos, R., and Cunningham, G. Magnetic resonance imaging in human pregnancy. *Obstet. Gynecol.* 66: 629-633 (1985).
18. Powell, M. C., Buckley, J., Price, H., Worthington, B. S., and Symonds, E. M. Magnetic resonance imaging and placenta previa. *Am. J. Obstet. Gynecol.* 154: 565-569 (1986).
19. Weinreb, J. C., Lowe, T. W., Santos-Ramos, R., Cunningham, F. G., and Parkey, R. Magnetic resonance imaging in obstetric diagnosis. *Radiology* 154: 157-161 (1985).
20. Mattison, D. R., Kay, H. H., and Heinrichs, W. L. The widening window of magnetic resonance imaging. *Contemp. Ob/Gyn* 10: 91-108 (1985).
21. Smith, F. W., Adam, A. H., and Phillips, W. D. P NMR imaging in pregnancy. *Lancet* i(8314-5): 61-62 (1983).
22. Weinreb, J. C., L., Mattison, D. R., Jordan, J., and Thomford, P. J. Effect of manganese on human placental spin-lattice ( $T_1$ ) and spin-spin ( $T_2$ ) relaxation times. *Physiol. Chem. Phys. Med. NMR* 18: 41-48 (1986).
23. Thomford, P. J., Jordan, J., Angtuaco, T., Cockrill, H. H., and Mattison, D. R. Characterization of magnetic resonance parameters in the pregnant uterus. *Trophoblast Res.* 2: 345-370 (1987).
24. Panigel, M., Coulam, C., Wolf, G., Zeleznik, A., Leone, F., and Podesta, C. Magnetic resonance imaging (MRI) of the placental circulation using gadolinium-DTPA as a paramagnetic marker in the Rhesus monkey *in vivo* and the perfused human placenta *in vitro*. *Trophoblast Res.* 3, in press.
25. Miller, R. K. Placental transfer and function: The interface for drugs and chemicals in the conceptus. In: *Drug and Chemical Action in Pregnancy: Pharmacologic and Toxicologic Principles* (S. Fabro and A. R. Scialli, Eds.), Marcel Dekker, Inc., New York, 1986, pp. 123-152.
26. Shah, Y. G., and Miller, R. K. The pharmacokinetics of phenytoin in the perfused human placenta. *Pediatr. Pharmacol.* 5: 165-179 (1985).
27. Wier, P. J., and Miller, R. K. The pharmacokinetics of cadmium in the dually perfused human placenta. *Trophoblast Res.* 2: 357-366 (1987).
28. Miller, R. K., Mattison, D. R., and Plowchalk, D. Biological monitoring of the human placenta. In: *Biological Monitoring of Metals* (T. W. Clarkson, G. Nordberg, and P. Sager, Eds.), Plenum Press, New York, in press.